Dalton Transactions

RSC Publishing

PERSPECTIVE

View Article Online
View Journal | View Issue

Cite this: *Dalton Trans.*, 2013, **42**, 15846

Long-lived photoinduced charge separation for solar cell applications in supramolecular complexes of multi-metalloporphyrins and fullerenes

Shunichi Fukuzumi*[a,b] and Kei Ohkubo[a]

Monomers, dimers, trimers, dendrimers and oligomers of metalloporphyrins form supramolecular complexes with fullerene derivatives *via* electrostatic interactions, π–π interactions and coordination bonds. Photoexcitation of the supramolecular complexes resulted in photoinduced electron transfer from the porphyrin moiety to the fullerene moiety to produce the charge-separated states as revealed by laser flash photolysis measurements. The rate constants of photoinduced charge separation and charge recombination in supramolecular complexes of multi-metalloporphyrins and fullerenes were also determined by laser flash photolysis measurements and the results depending on the number of porphyrins in the supramolecular complexes are discussed in terms of efficiency of photoinduced energy transfer and charge separation as well as the lifetimes of charge-separated states. The photoelectrochemical performances of solar cells composed of supramolecular complexes of monomers, dimers, dendrimers and oligomers of metalloporphyrins with fullerenes are compared in relation to the rate constants of photoinduced charge separation and charge recombination.

Received 12th July 2013,
Accepted 3rd October 2013

DOI: 10.1039/c3dt51883c

www.rsc.org/dalton

1. Introduction

Photosynthesis is one of the most fundamental and indispensable processes in nature, because it converts light energy into chemical energy required to maintain life.[1,2] Photosynthesis is initiated by the multistep electron-transfer reactions in the photosynthetic reaction centres following light energy harvesting by antenna chlorophylls, funnelled to a bacteriochlorophyll

[a]*Department of Material and Life Science, Division of Advanced Science and Biotechnology, Graduate School of Engineering, Osaka University, ALCA, Japan Science and Technology Agency (JST), Suita, Osaka 565-0871, Japan. E-mail: fukuzumi@chem.eng.osaka-u.ac.jp; Fax: +81-6-6879-7370; Tel: +81-6-6879-7368*

[b]*Department of Bioinspired Science, Ewha Womans University, Seoul 120-750, Korea*

Shunichi Fukuzumi

Shunichi Fukuzumi earned a Ph.D. degree in applied chemistry at the Tokyo Institute of Technology in 1978. After working as a postdoctoral fellow (1978–1981) at Indiana University in USA, he joined the Department of Applied Chemistry, Osaka University, as an Assistant Professor in 1981 and was promoted to a Full Professor in 1994. He is now a special distinguished professor at Osaka University and the director of an ALCA (Advanced Carbon Technology Research and Development) project that started in 2011.

Kei Ohkubo

Kei Ohkubo earned his Ph.D. degree from the Graduate School of Engineering, Osaka University in 2001. He was working as a JSPS fellow and a JST research fellow at Osaka University from 2001 to 2005. He has been a designated associate professor at Osaka University since 2005.

dimer, the so-called special pair, to attain the long-lived charge-separated (CS) state.[1,2] The redox-active components such as chlorophyll, pheophytin and quinones are appropriately located in the protein matrix by non-covalent interactions.[1,2] Extensive efforts have so far been devoted to the design of electron donor–acceptor composites using covalently and non-covalently linked systems to form the long-lived CS state upon photoexcitation for artificial photosynthesis.[3–29] Porphyrins, which are involved in a number of important biological electron-transfer systems including the primary photochemical reactions of chlorophylls (porphyrin derivatives) in the photosynthetic reaction centres, are particularly attractive building blocks as electron acceptors as well as light-harvesting compounds for the construction of supramolecular electron donor–acceptor composites due to their excellent photophysical and electron-transfer properties.[8–29] With regard to electron acceptors, fullerenes, which are extensively conjugated three-dimensional π systems, are ideal electron acceptors because of the minimal changes of structure and solvation associated with the electron-transfer reduction.[30–38] Thus, combination of porphyrins and fullerenes is regarded as ideal donor–acceptor ensembles, because the combination results in a small reorganization energy, which allows to accelerate photoinduced electron transfer and to slow down charge recombination, leading to the generation of long-lived CS states with high quantum yields.[39–63] However, non-covalent binding between monomer porphyrins and fullerenes is usually not strong enough in polar solvents which are generally used for studies on photoinduced electron-transfer reactions.[64–68] Among non-covalent interactions, an electrostatic interaction is relatively strong in polar solvents.[69–73] Muti-point binding sites can be introduced by using multi-metalloporphyrins (dimers, trimers, dendrimers and oligomers), allowing strong binding between multi-metalloporphyrins and fullerenes in polar solvents.[29,30]

In this perspective, we review our recent development on photoinduced charge separation in supramolecular complexes of porphyrin anions and fullerene cations with electrostatic interactions and those composed of multi-metalloporphyrins and fullerenes, which are strongly bound in polar solvents, towards construction of supramolecular solar cells based on the long-lived photoinduced charge separation.

2. Supramolecular complexes of monomer porphyrin sulfonates and $Li^+@C_{60}$

Zinc tetraphenylporphyrin tetrasulfonate anion $[(Bu_4N^+)_4ZnTPPS^{4-}]$ forms a strong supramolecular binding with a cationic lithium ion encapsulated fullerene $(Li^+@C_{60})$[74–77] in benzonitrile (PhCN) by electrostatic and π–π interactions (Scheme 1).[78] The Job's plots of the absorbance change confirmed the 1 : 1 stoichiometry between $ZnTPPS^{4-}$ and $Li^+@C_{60}$.[78] Free base tetraphenylporphyrin tetrasulfonate anion $[(Bu_4N^+)_4H_2TPPS^{4-}]$ also forms a 1 : 1 complex with $Li^+@C_{60}$. The formation constants (K) of the $ZnTPPS^{4-}/Li^+@C_{60}$ and $H_2TPPS^{4-}/Li^+@C_{60}$ complexes were determined from the absorption change to be 1.6×10^5 and 3.0×10^5 M^{-1}, respectively.[78] The same formation constants were obtained from the fluorescence quenching of $ZnTPPS^{4-}$ and H_2TPPS^{4-} and by $Li^+@C_{60}$ in PhCN.[78]

The occurrence of the photoinduced energy transfer in the supramolecular complex was confirmed by the transient absorption spectra of the $ZnTPPS^{4-}$–$Li^+@C_{60}$ complex measured in PhCN using femtosecond laser flash photolysis (Fig. 1a).[78] The transient absorption bands taken at 2 ps observed at 620 and 737 nm are assigned to the singlet excited state of $ZnTPPS^{4-}$. This band decays with the rate constant (k_{EN}) of 9.7×10^{10} s^{-1} (Fig. 1b) to form the singlet excited state of $Li^+@C_{60}$ at 100 ps (Fig. 1a). The decay rate constant of $^1[Li^+@C_{60}]^*$ was determined to be 8.9×10^8 s^{-1}, which agrees with the rate constant of the intersystem crossing of $Li^+@C_{60}$.[78] Thus, efficient energy transfer occurred from $^1[ZnTPPS^{4-}]^*$ to $Li^+@C_{60}$ rather than electron transfer.

The transient absorption spectra taken by nanosecond laser flash photolysis shown in Fig. 2a demonstrate the formation of $[ZnTPPS^{4-}]^{\bullet+}$ (λ_{max} = 670 nm) and that of $Li^+@C_{60}$ radical anion (λ_{max} = 1035 nm).[78] Thus, the electron transfer from

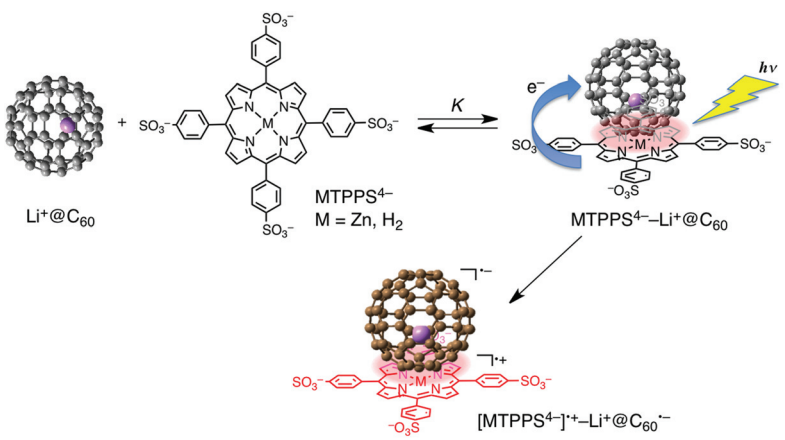

Scheme 1 Supramolecular complex formation and photoinduced charge separation of $MTPPS^{4-}$ (M = Zn and H_2) with $Li^+@C_{60}$ in PhCN.

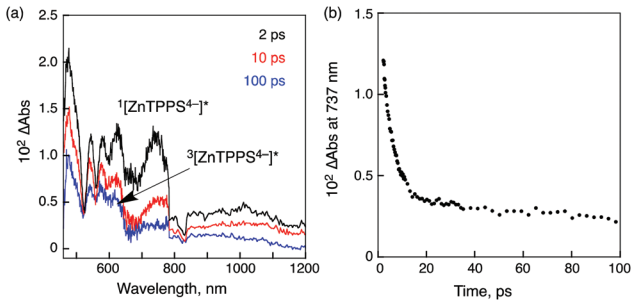

Fig. 1 (a) Transient absorption spectra of ZnTPPS^{4-} (2.5×10^{-5} M) in the presence of Li$^+$@C$_{60}$ (5.0×10^{-5} M) in deaerated PhCN at 298 K taken at 2, 10 and 100 ps after femtosecond laser excitation at 388 nm. (b) Time profile at 737 nm.

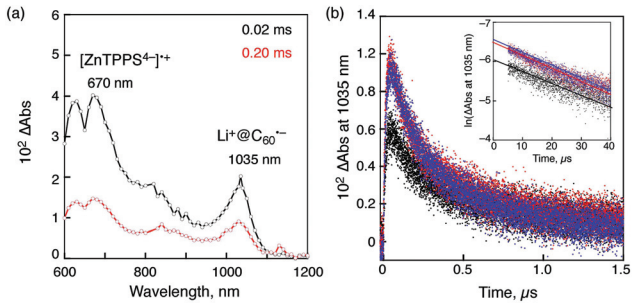

Fig. 2 (a) Transient absorption spectra of ZnTPPS^{4-} (2.5×10^{-5} M) in the presence of Li$^+$@C$_{60}$ (5.0×10^{-5} M) in deaerated PhCN at 298 K taken at 20 and 200 μs after nanosecond laser excitation at 550 nm; (b) decay time profiles at 1035 nm with different laser intensities (1, 3, 6 mJ per pulse). Inset: first-order plots.

ZnTPPS^{4-} to ^{3}[Li$^+$@C$_{60}$]* or from ^{3}[ZnTPPS^{4-}]* to Li$^+$@C$_{60}$ occurs in the supramolecular complex to produce the triplet charge-separated (CS) state. The lifetime of the triplet CS state of the supramolecular complex was determined to be 300 μs for ZnTPPS^{4-} from the first-order decay of the CS state (Fig. 2b).[78] It was confirmed that back electron transfer occurred in the supramolecular complex, because the first-order decay rate constant remains the same irrespective of the difference in the laser intensity (inset of Fig. 2b).[78] Similarly the CS lifetime of 310 μs was determined for [(H$_2$TPPS^{4-})$^{\bullet+}$–Li$^+$@C$_{60}^{\bullet-}$].[78] This is the longest lifetime of the CS state ever reported for monomer porphyrin/fullerene systems linked non-covalently in solution. The quantum yield of the CS state is determined to be 0.39 using the absorption of the CS state (Li$^+$@C$_{60}^{\bullet-}$: ε_{1035} = 7300 M^{-1} cm^{-1}).[78]

The activation enthalpies of the charge-recombination (CR) processes were determined to be 3.0 kcal mol^{-1} for ZnTPPS^{4-}–Li$^+$@C$_{60}$ and 5.4 kcal mol^{-1} for H$_2$TPPS^{4-}–Li$^+$@C$_{60}$.[78] This indicates that there is a significant energy difference between the singlet and triplet CS states and that the CR processes may occur through the thermally activated singlet CS state. The lifetime of the CS state at 77 K is estimated as long as 60 h for H$_2$TPPS^{4-}–Li$^+$@C$_{60}$.[78] Such a long-lived triplet CS state was detected by the EPR measurements by photoirradiation of the H$_2$TPPS^{4-}–Li$^+$@C$_{60}$ complex in frozen PhCN as shown in

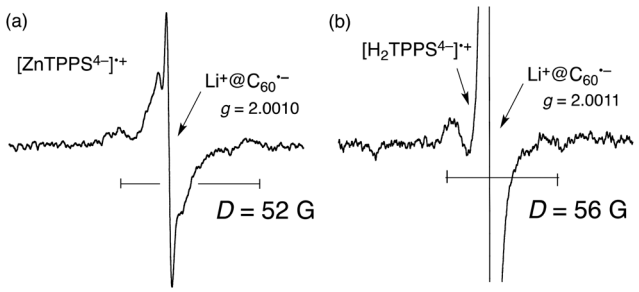

Fig. 3 EPR spectra of (a) (ZnTPPS^{4-})$^{\bullet+}$–Li$^+$@C$_{60}^{\bullet-}$ and (b) (H$_2$TPPS^{4-})$^{\bullet+}$–Li$^+$@C$_{60}^{\bullet-}$ in PhCN generated by photoirradiation with a high-pressure Hg lamp (1000 W) at 77 K.

Fig. 3. The spin–spin interaction in the triplet radical ion pair of the supramolecular complex is clearly shown at 77 K, where the fine structure due to the triplet CS state is clearly observed at g = 2. From the zero-field splitting values (D = 52 G for ZnTPPS^{4-} and 56 G for H$_2$TPPS^{4-}) the distances (r) between two electron spins were estimated using the relation, D = 27 800/r^3,[79,80] to be 8.1 and 7.9 Å, respectively.[78] These r values agree with the centre-to-centre distance of a reported crystal structure of porphyrin/C$_{60}$.

By mixing PhCN solutions of the supramolecular complexes of MTPPS^{4-} and Li$^+$@C$_{60}$ with acetonitrile (MeCN), nanoclusters were produced and they were deposited on an optically transparent electrode (OTE) of nanostructured SnO$_2$ (OTE/SnO$_2$) by application of a dc electric field (~100 V cm^{-1}) to construct photovoltaic cells.[81] The (MTPPS^{4-}/Li$^+$@C$_{60}$)$_n$ films are composed of closely packed Li$^+$@C$_{60}$ clusters of about 80 nm size, which render a nanoporous morphology to the film as shown in the TEM images in Fig. 4.[81]

The photoelectrochemical measurements of a robust thin film of OTE/SnO$_2$/(MTPPS^{4-}/Li$^+$@C$_{60}$)$_n$ were performed using a standard two-electrode system consisting of a working electrode and a Pt wire gauze electrode in air-saturated MeCN containing 0.5 M LiI and 0.01 M I$_2$ (Fig. 5).[77] The IPCE (incident photon-to-photocurrent efficiency) values were determined by normalizing the photocurrent values for incident light energy and intensity and using eqn (1).[82–85]

$$\text{IPCE}\ (\%) = 100 \times 1240 \times i_{sc}/(I_{inc} \times \lambda) \qquad (1)$$

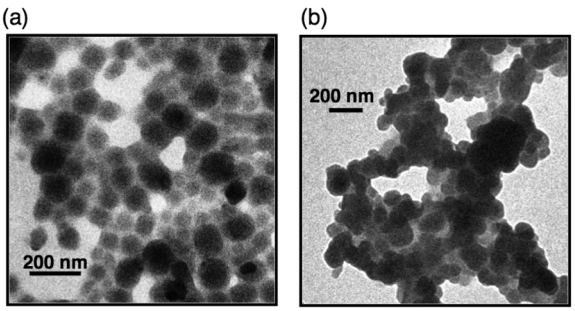

Fig. 4 TEM images of (a) Li$^+$@C$_{60}$/ZnTPPS^{4-} and (b) Li$^+$@C$_{60}$/H$_2$TPPS^{4-} nanoclusters.

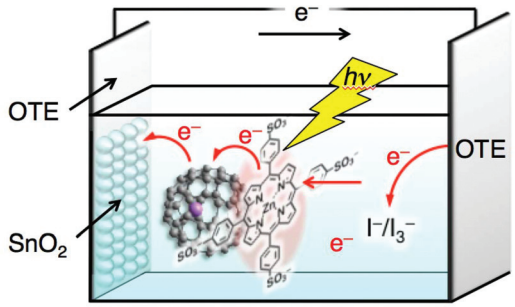

Fig. 5 Schematic image of photoelectrochemical cell of OTE/SnO_2/$MTPPS^{4-}$/$Li^+@C_{60}$ and electron-transfer pathways to generate photocurrent.

where i_{sc} is the short circuit photocurrent (A cm^{-2}), I_{inc} is the incident light intensity (W cm^{-2}) and λ is the wavelength (nm). The IPCE value of OTE/SnO_2/$(ZnTPPS^{4-}/Li^+@C_{60})_n$ is much higher than the sum of the two individual IPCE values of the individual systems OTE/SnO_2/$(ZnTPPS^{4-})_n$ and OTE/SnO_2/$(Li^+@C_{60})_n$ in the visible region (Fig. 6). The maximum IPCE value of OTE/SnO_2/$(ZnTPPS^{4-}/Li^+@C_{60})_n$ was 77% at 450 nm. Such a high IPCE value indicates that photocurrent generation is initiated *via* photoinduced electron transfer from $ZnTPPS^{4-}$ to $Li^+@C_{60}$, followed by the charge transport to the collective surface of an OTE/SnO_2 electrode (Fig. 5). When $ZnTPPS^{4-}$ was replaced by H_2TPPS^{4-}, a significantly low IPCE value was observed as 7% at 440 nm probably because of the self-aggregation of H_2TPPS^{4-} without binding with $Li^+@C_{60}$.[81]

The power conversion efficiency (η) of the OTE/SnO_2/$(ZnTPPS^{4-}/Li^+@C_{60})_n$ electrode was calculated by using eqn (2):[82–85]

$$\eta = \mathrm{FF} \times I_{sc} \times V_{oc}/W_{in} \quad (2)$$

in which the fill factor (FF) is defined as FF = $[IV]_{max}/I_{sc}V_{oc}$ and V_{oc} is the open-circuit photovoltage and I_{sc} is the short-circuit photocurrent. The OTE/SnO_2/$(ZnTPPS^{4-}/Li^+@C_{60})_n$ electrode has an overall power conversion efficiency (η) of 2.1% at an input power (W_{in}) of 28 mW cm^{-2}, whereas FF = 0.37, V_{oc} = 460 mV and I_{sc} = 3.4 mA cm^{-2} in the OTE/SnO_2/$(ZnTPPS^{4-}/Li^+@C_{60})_n$. The η value is two orders of magnitude greater than that of the previously reported simple porphyrin and C_{60} composite system (~0.03%).[83] Such a significant enhancement of the η value indicates that the strong ordering in the clusters and the efficient charge separation in $(ZnTPPS^{4-}/Li^+@C_{60})_n$ improved the light energy conversion properties.

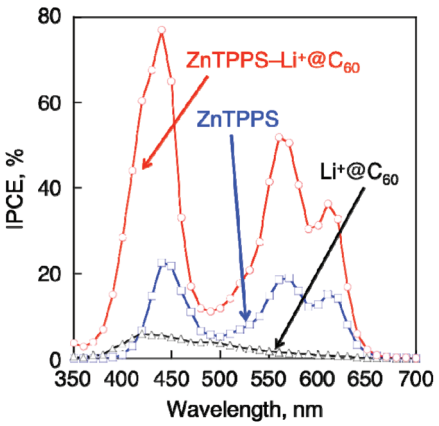

Fig. 6 Photocurrent action spectra of OTE/SnO_2/$(ZnTPPS^{4-}/Li^+@C_{60})_n$ (red) OTE/SnO_2/$(ZnTPPS^{4-})_n$ (blue) and OTE/SnO_2/$(Li^+@C_{60})_n$ (black). Electrolyte: 0.5 M LiI and 0.01 M I_2 in MeCN–PhCN (3 : 1 v/v).

3. Supramolecular complexes of cyclic porphyrin dimers with C_{60} and $Li^+@C_{60}$

As compared to porphyrin monomers, porphyrin dimers with appropriate linkage can accommodate electron acceptor guest molecules by π–π interactions to form sandwich complexes.[86–96] For example, a cyclic Ni porphyrin dimer (Ni-CPD_{Py}) linked by butadiyne moieties bearing 4-pyridyl groups (Fig. 7) forms a sandwich complex with C_{60} ($C_{60} \subset Ni_2$-CPD_{Py}) as shown in the X-ray crystal structure (Fig. 8), where the dimer bites a C_{60} molecule by tilting the porphyrin rings with respect to each other and there are strong π–π interactions between the porphyrin rings and C_{60}.[97] The adjacent dimers are linked by hydrogen bonds and π–π interactions.[97] The C_{60} molecules are linearly arranged in the inner channel to give a supramolecular peapod.[97–102]

The linear arrangement of C_{60} in $C_{60} \subset Ni_2$-CPD_{Py} high electron mobilities of $\sum\mu$ = 0.72 and 0.20 $cm^2\ V^{-1}\ s^{-1}$ along the *b* and *c* axes, respectively, which were determined by flash-photolysis time-resolved microwave conductivity (FP-TRMC) measurements.[97] The TRMC technique can evaluate the

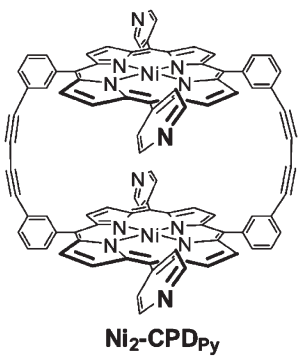

Fig. 7 Chemical structure of Ni_2-CPD_{Py}.

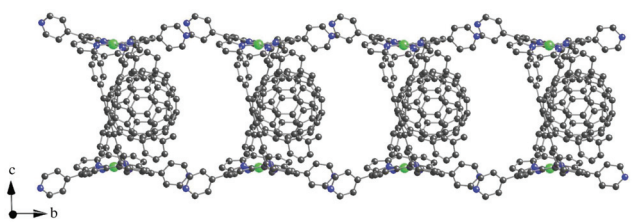

Fig. 8 Crystal structures of tubular assemblies of $C_{60} \subset Ni_2$-CPD_{Py}. Hydrogen atoms are omitted for clarity.

intrinsic mobility without being affected by the chemical or physical defects in the material and/or the organic/metal–electrode interfaces.[103–105] The observed value along the *b* axis of the single crystal of $C_{60} \subset Ni_2\text{-}CPD_{Py}$ is comparable to that of the single crystal of C_{60} ($\sum\mu$ = 0.50 $cm^2\ V^{-1}\ s^{-1}$ measured by TOF).[106] The observed high electron mobility along the *b* axis is due to the well-ordered linear arrangement of C_{60} in the porphyrin nanotube. However, the expected charge-separated state could not be observed in the time-resolved transient absorption spectra of $C_{60} \subset Ni_2\text{-}CPD_{Py}$ because the singlet excited state of the nickel porphyrin immediately changes to the triplet excited state by intersystem crossing and the low energy triplet excited state of C_{60} ($^3C_{60}$*) is formed by energy transfer.[97] The estimated energy level of the charge-separated state (1.98 eV) is higher than that of $^3C_{60}$* (1.60 eV).[97] When $Ni_2\text{-}CPD_{Py}$ was replaced by a free base porphyrin dimer (H4-CPDPy), a complete charge-separated state {$H_4\text{-}CPDPy^{\bullet+}$ + $C_{60}^{\bullet-}$)} was observed by femtosecond laser flash photolysis of $C_{60} \subset H_4\text{-}CPD_{Py}$ in the solid state with a lifetime of 470 ps.[107] The photovoltaic activity of $C_{60} \subset Ni_2\text{-}CPD_{Py}$ and $C_{60} \subset H_4\text{-}CPD_{Py}$ was evaluated by using solar cells composed of modified electrodes and I^-/I_3^- solution.[107] The $C_{60} \subset H_4\text{-}CPD_{Py}$-modified electrode exhibited IPCE of 17% and a power conversion efficiency (η) of 0.33%, which was more than 16 times larger than that of $OTE/SnO_2/(C_{60} \subset Ni_2\text{-}CPD_{Py})_n$ (0.02%).[107] Such a significant enhancement of the η value demonstrates that the formation of highly ordered clusters and the efficient charge separation of $(C_{60} \subset H_4\text{-}CPD_{Py})_n$ contributes to the improvement of the light energy conversion properties.[107]

When C_{60} is replaced by $Li^+@C_{60}$, porphyrin dimers with four long alkoxy substituents on the *meso*-phenyl groups ($MCPD_{Py}(OC_6)$ in Fig. 9) form strong supramolecular complexes in even a polar solvent such as PhCN.[108] The association constants (K_{assoc}) of $Li^+@C_{60} \subset MCPD_{Py}(OC_6)$ in PhCN at 298 K were determined to be $2.6 \times 10^5\ M^{-1}$ for $Li^+@C_{60} \subset H_4\text{-}CPD_{Py}(OC_6)$ and $3.5 \times 10^5\ M^{-1}$ for $Li^+@C_{60} \subset Ni_2\text{-}CPD_{Py}(OC_6)$.[108]

Upon laser excitation of $Li^+@C_{60} \subset Ni_2\text{-}CPD_{Py}(OC_6)$, transient absorption bands due to $Ni_2\text{-}CPD_{Py}(OC_6)^{\bullet+}$ and $Li^+@C_{60}^{\bullet-}$ were observed as shown in Fig. 10a.[108] In this case, electron

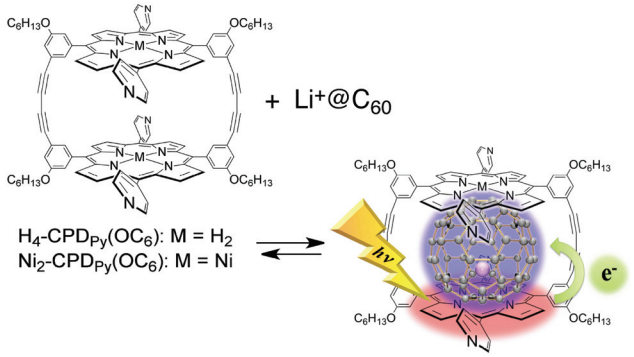

Fig. 9 Supramolecular formation and photoinduced charge separation between $MCPD_{Py}(OC_6)$ and $Li^+@C_{60}$.

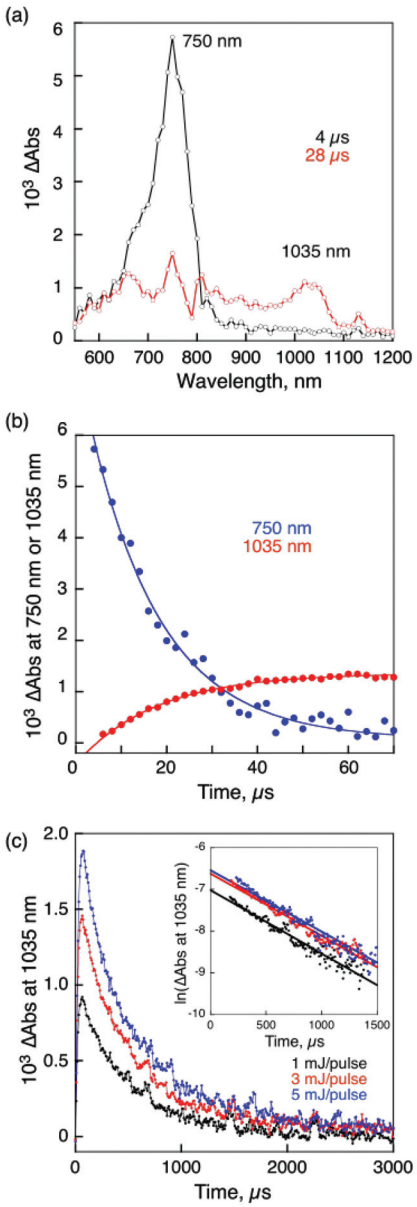

Fig. 10 (a) Transient absorption spectra of $Ni_2\text{-}CPD_{Py}(OC_6)$ with $Li^+@C_{60}$ in deaerated PhCN at room temperature taken at 4 and 28 μs after nanosecond laser excitation at 520 nm. [$Ni_2\text{-}CPD_{Py}(OC_6)$] = 2.5×10^{-5} M, [$Li^+@C_{60}$] = 5.0×10^{-5} M. (b) Rise and (c) decay time profiles at 1035 nm with different laser intensities (1, 3, 5 mJ per pluse). Inset: first-order plots.

transfer occurs from $Ni_2\text{-}CPD_{Py}(OC_6)$ to the triplet excited state of $Li^+@C_{60}$ ($^3Li^+@C_{60}$*) rather than from $^3[Ni_2\text{-}CPD_{Py}(OC_6)]$* to $Li^+@C_{60}$ as indicated by the disappearance of the absorption band at 750 nm due to $^3Li^+@C_{60}$*, accompanied by the appearance of the absorption band at 1035 nm due to $Li^+@C_{60}^{\bullet-}$ (Fig. 10b).[108] The rate constant of electron transfer from $Ni_2\text{-}CPD_{Py}(OC_6)$ to $^3Li^+@C_{60}$* to produce the CS state was determined from the rise in the absorbance at 1035 nm due to $Li^+@C_{60}^{\bullet-}$ to be $5.7 \times 10^7\ s^{-1}$.[108] The absorbance at 1035 nm due to $Li^+@C_{60}^{\bullet-}$ in the CS state decayed obeying first-order kinetics with the same slope irrespective of the difference in

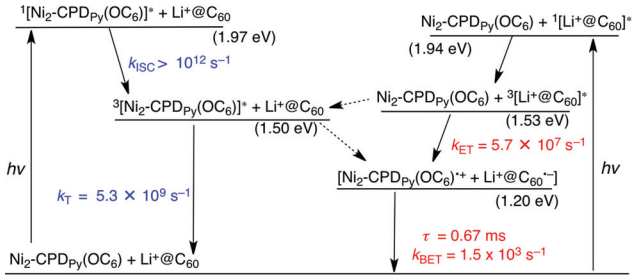

Scheme 2 Energy diagram for Li$^+$@C$_{60}$ ⊂ Ni$_2$-CPD$_{Py}$(OC$_6$); broken arrow: minor pathway.

the laser intensity (Fig. 10c).[108] This clearly indicates that the decay of the CS state occurs *via* intrasupramolecular back electron transfer rather than a bimolecular back electron-transfer reaction between the CS states. The CS lifetime was determined from the slope of the first-order plots in Fig. 10c to be 0.67 ms, which is the longest value ever reported for non-covalent monomer dimer porphyrin-fullerene supramolecules in solution.[108] The CS state was also observed for Li$^+$@C$_{60}$ ⊂ H$_4$-CPD$_{Py}$(OC$_6$). The quantum yields of the CS states were estimated to be 0.13 for Li$^+$@C$_{60}$ ⊂ Ni$_2$-CPD$_{Py}$(OC$_6$) and 0.32 for Li$^+$@C$_{60}$ ⊂ H$_4$-CPD$_{Py}$(OC$_6$) and by means of the comparative method with the absorption intensities of the CS states (Li$^+$@C$_{60}^{\bullet-}$: ε(1035 nm) = 7300 M^{-1} cm^{-1}).[108] When Li$^+$@C$_{60}$ was replaced by pristine C$_{60}$, no CS states were produced as predicted by their higher energy levels than those of the triplet excited states of CPD$_{Py}$(OC$_6$) and C$_{60}$.[108]

The mechanisms of intrasupramolecular photoinduced charge separation in Li$^+$@C$_{60}$ ⊂ Ni$_2$-CPD$_{Py}$(OC$_6$) are shown in Scheme 2.[108] The singlet excited state of Ni$_2$-CPD$_{Py}$(OC$_6$) (^{1}[Ni$_2$-CPD$_{Py}$(OC$_6$)]*) is generated upon photoexcitation of Li$^+$@C$_{60}$ ⊂ Ni$_2$-CPD$_{Py}$(OC$_6$) at 420 nm, where the porphyrin moiety is exclusively excited. Even if the Li$^+$@C$_{60}$ moiety is excited, energy transfer from ^{1}[Li$^+$@C$_{60}$]* (E_s = 1.94 eV)[77] to Ni$_2$-CPD$_{Py}$(OC$_6$) (E_s = 1.97 eV) occurs to produce ^{1}[Ni$_2$-CPD$_{Py}$(OC$_6$)]*. Although electron transfer from ^{1}[Ni$_2$-CPD$_{Py}$(OC$_6$)]* to Li$^+$@C$_{60}$ is energetically possible (Scheme 2), the fast intersystem crossing occurs to generate ^{3}[Ni$_2$-CPD$_{Py}$(OC$_6$)]* (k_{ISC} > 10^{12} s^{-1}).[108] Then, electron transfer occurs from ^{3}[Ni$_2$-CPD$_{Py}$(OC$_6$)]* to Li$^+$@C$_{60}$ with the driving force of 0.30 eV to produce the CS state. The CS state decays slowly *via* intrasupramolecular BET with the lifetime of 0.67 ms (Scheme 2).[108]

4. Supramolecular complex of a porphyrin tripod with C$_{60}$

The tripod conformation of a porphyrin trimer (TPZn$_3$) in Fig. 11 makes it possible to capture a fullerene derivative containing a pyridine moiety (PyC$_{60}$)[109] inside the cavity strongly by π–π interactions together with the coordination bond between Zn^{2+} and the pyridine moiety (Scheme 3).[110–113] The association constant of TPZn$_3$ with PyC$_{60}$ (1.1 × 10^5 M^{-1} in

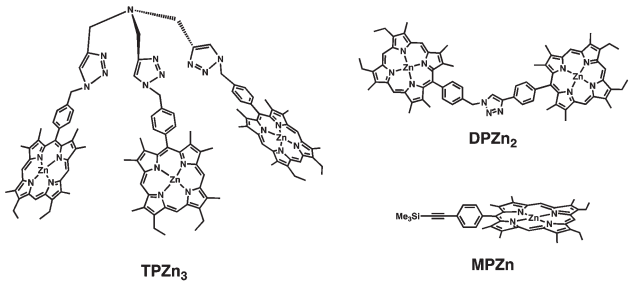

Fig. 11 A porphyrin tripod and the reference dimer and monomer.

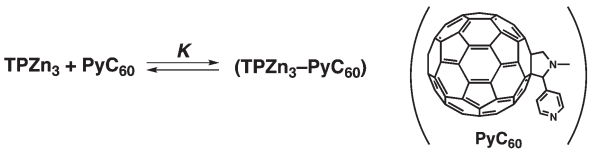

Scheme 3 Formation of a supramolecular complex between TPZn$_3$ and PyC$_{60}$.

toluene) determined from the UV-vis absorption spectral titration (Fig. 12a) is much larger as compared with those of the corresponding monomer (MPZn) and dimer porphyrin (DPZn$_2$).[109] The ^{1}H NMR signals of TPZn$_3$ exhibit downfield shifts upon complexation with PyC$_{60}$, whereas the pyridyl protons of PyC$_{60}$ exhibit large upfield shifts by the complexation, which is ascribed to the influence of the large porphyrin aromatic ring current.[113] This result clearly shows that the

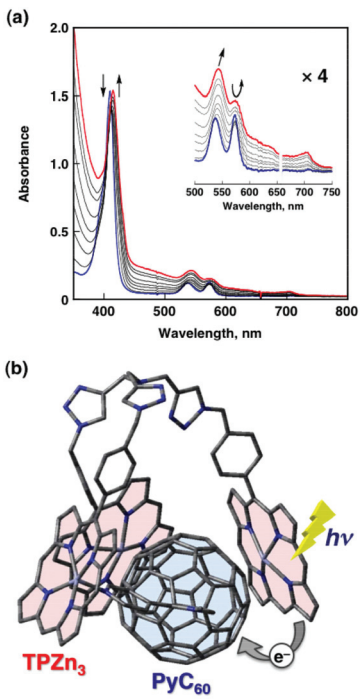

Fig. 12 (a) UV-Vis spectral changes upon addition of PyC$_{60}$ (0 to 48 μM) to an *o*-DCB solution of TPZn$_3$ (3 μM) at 298 K. (b) Schematic view of photoinduced electron transfer in the TPZn$_3$–PyC$_{60}$ complex. The structure of the TPZn$_3$–PyC$_{60}$ complex was optimized by DFT at the B3LYP/3-21G(*) level.

pyridyl group of PyC_{60} coordinates to the central zinc ions of $TPZn_3$. The encapsulation of PyC_{60} into the cavity of $TPZn_3$ was supported by the DFT-optimized structure (B3LYP/3-21G(*) basis set) in Fig. 12b.[113]

The occurrence of photoinduced electron transfer from $^1TPZn_3$* to PyC_{60} was confirmed by femtosecond laser flash photolysis measurements in Fig. 13a, where the transient absorption spectrum due to $^1TPZn_3$* changes as time elapses to afford the absorption bands at λ_{max} = 1000 nm due to the monofunctionalized fullerene radical anion[114,115] and at 670 nm due to the one-electron oxidized species of $TPZn_3$ ($TPZn_3^{\bullet+}$).[113,116,117]

In sharp contrast to the $TPZn_3$–PyC_{60} complex, the transient absorption spectrum of the monomer porphyrin (MPZn) in the presence of PyC_{60} (Fig. 13b) exhibits the absorbance change due to the energy transfer from ^{1}MPZn* to PyC_{60} to give the singlet excited state $^1PyC_{60}$* (1.76 eV), followed by the conversion to the triplet excited states ^{3}MPZn* and $^3PyC_{60}$* at 2800 ps (green line in Fig. 13b), accompanied by the recovery of the ground state.[113]

The energy diagrams of photodynamics for $TPZn_3$ and MPZn in the presence of PyC_{60} in toluene are shown in Scheme 4a and 4b, respectively.[113] The energy level (1.49 eV) of the CS state ($TPZn_3^{\bullet+}$–$PyC_{60}^{\bullet-}$) is lower than the energy level of the triplet excited state of PyC_{60} moieties (1.56 eV). The rate constant (k_{ET}) of photoinduce electron transfer from $^1TPZn_3$* to PyC_{60} is larger than the rate constant of intersystem crossing. From the rate constant of back electron transfer (k_{BET} = 1.9×10^9 s^{-1}), the lifetime of the CS state is determined to be τ_{CS} = 0.53 ns. In contrast, only energy transfer from ^{1}MPZn* to PyC_{60} occurs to produce $^1PyC_{60}$*, in competition with intersystem crossing to ^{3}MPZn*.[113]

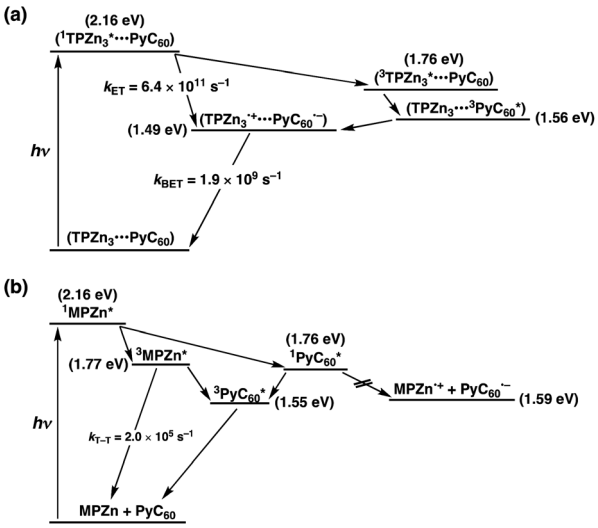

Scheme 4 Energy diagrams for photodynamics of (a) $TPZn_3$ and (b) MPZn in the presence of PyC_{60} in toluene.

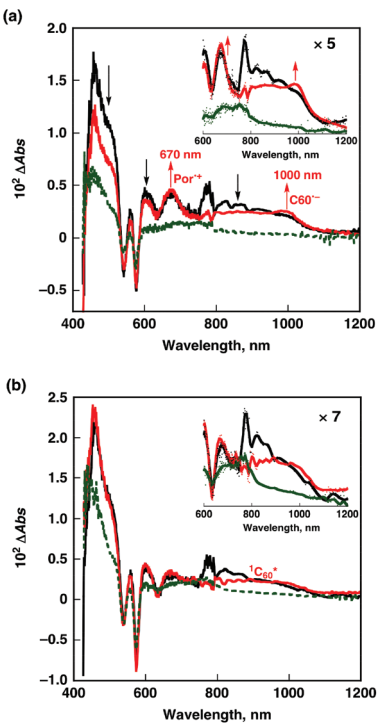

Fig. 13 Transient absorption spectra of (a) $TPZn_3$ (7.0×10^{-6} M) and (b) MPZn (1.1×10^{-5} M) in the presence of PyC_{60} (2.3×10^{-5} M) obtained at 2 ps (black), 62 ps (red), and 2800 ps (green) after femtosecond laser pulse irradiation at 410 nm in deaerated toluene at 298 K.

$TPZn_3$ also forms a stable 1 : 1 complex with gold(III) tetra(4-pyridyl)porphyrin ($AuTPyP^+$) in nonpolar solvents.[118] The strong binding of $TPZn_3$ with $AuTPyP^+$ results from the encapsulation of $AuTPyP^+$ inside the cavity of $TPZn_3$ through multiple coordination bonds. The efficient quenching of the singlet excited state of $TPZn_3$ occurs *via* a photoinduced electron-transfer pathway in the $TPZn_3$–$AuTPyP^+$ complex as the case of $TPZn_3$–PyC_{60} complex.[118]

5. Supramolecular complexes of porphyrin oligopeptides and C_{60}

Multiple photosynthetic reaction centres composed of light-harvesting multiporphyrin units and charge-separation units were obtained by using both the coordination bond and π–π interaction. Zinc porphyrinic oligopeptides with various numbers of porphyrin units [$P(ZnP)_n$; n = 2, 4, 8][119,120] were used as light-harvesting multiporphyrin units (Fig. 14), which are bound to electron acceptors of fulleropyrrolidine bearing a pyridine (PyC_{60})[113] or imidazole coordinating ligand (ImC_{60})[82] as shown in Fig. 15.[121]

The binding constant (K) of PyC_{60} to $P(ZnP)_n$ increased with increasing number of zinc porphyrins in an oligopeptide unit.[121] No supramolecular complex formation was observed in the case of zinc tetraphenylporphyrin in PhCN.[121] The strong binding between $P(ZnP)_8$ and PyC_{60} results from the strong π–π interactions between two zinc porphyrins and PyC_{60} in addition to the axial coordination of PyC_{60} to zinc ions of the porphyrins. In the case of ImC_{60}, however, the highest K value was obtained in the $P(ZnP)_4$–ImC_{60} complex. This

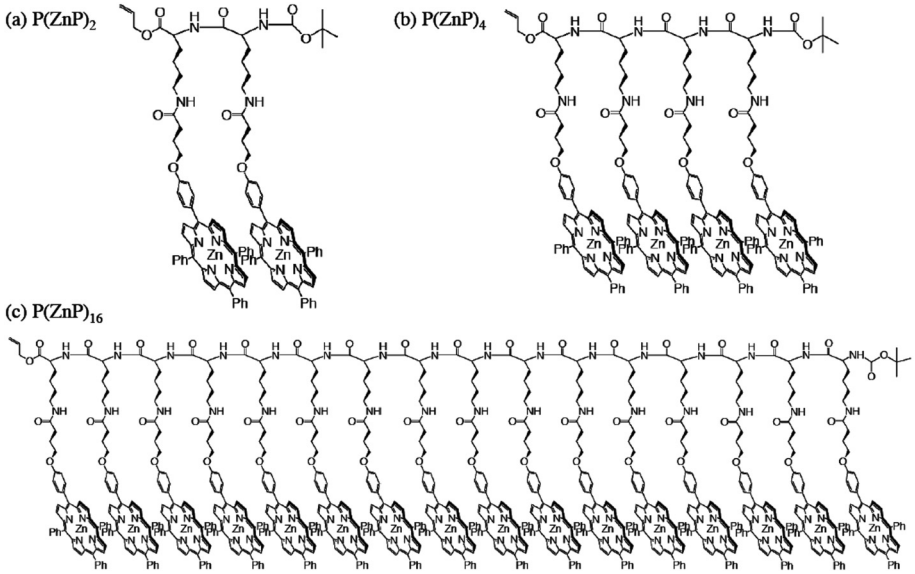

Fig. 14 Chemical structures of $P(ZnP)_2$, $P(ZnP)_4$ and $P(ZnP)_{16}$.

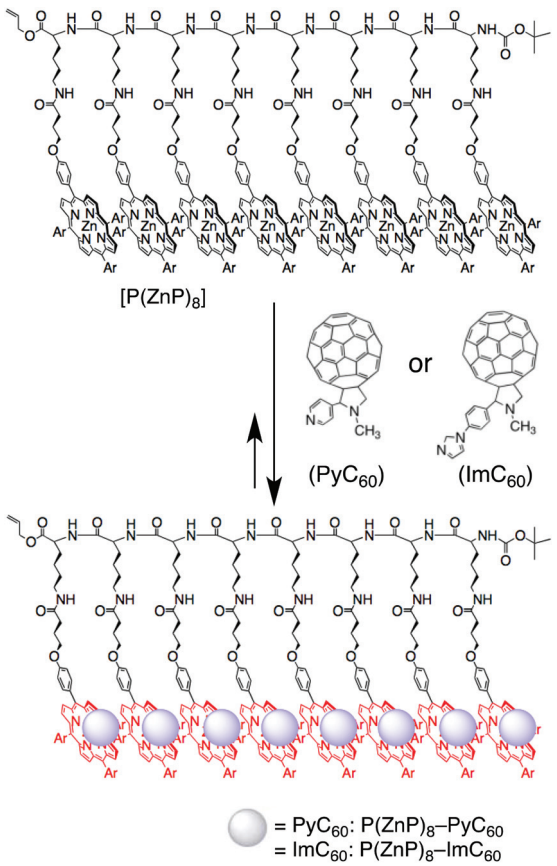

Fig. 15 Illustration of supramolecular complex composed of porphyrin-peptide octamer [$P(ZnP)_8$, Ar = 3,5-(*t*-Bu)$_2$C$_6$H$_3$] and PyC_{60} or ImC_{60}.

indicates that ImC_{60} is much more strongly bound by the oligopeptide, $P(ZnP)_4$, than PyC_{60}.[121] The apparent binding constants (K) determined from the fluorescence quenching of $P(ZnP)_n$ were significantly larger than those determined from the UV-vis spectral change, and the difference in the values increased with increasing the generation of porphyrinic oligopeptides (with increasing the number of the porphyrin units).[121] This indicates that the excited energy migration between the porphyrin units occurs efficiently prior to the electron transfer to the bound C_{60} moiety. An extremely efficient energy transfer also occurs in $P(ZnP)_8$–ImC_{60} judging from the large difference in the K values determined by the absorption change and by the fluorescence quenching (1.5×10^4 *vs.* 3.3×10^5 M^{-1}).

The occurrence of photoinduced electron transfer in the supramolecular complex in PhCN was confirmed by the transient absorption spectra of the supramolecular complex of $P(ZnP)_8$ with PyC_{60} using nanosecond laser flash photolysis.[121] The laser photoexcitation at 561 nm of the supramolecular complex of $P(ZnP)_8$ with PyC_{60} results in formation of the CS state as indicated by the transient absorption spectra in Fig. 16a, where the absorption band due to $PyC_{60}^{\bullet-}$ is clearly observed at 1000 nm together with that due to $ZnP^{\bullet+}$ at 630 nm.[121] The CS state detected decays obeying first-order kinetics (Fig. 16b) and the first-order plots at different initial CS concentrations afford linear correlations with the same slope (inset of Fig. 16b).[121] If there is any contribution of *intermolecular* back electron transfer from unbound $PyC_{60}^{\bullet-}$ to $ZnP^{\bullet+}$, the second-order kinetics would be involved for the decay time profile. In fact, the corresponding second-order plots (Fig. 16c) are clearly non-linear and the initial slope varies depending on the CS concentration. Thus, the decay process is ascribed to back electron transfer in the supramolecular complex rather than intermolecular back electron transfer between $ZnP^{\bullet+}$ and $PyC_{60}^{\bullet-}$.[121] The CS lifetimes of the supramolecular complexes of other porphyrins [$P(ZnP)_n$] and the fullerene derivative (ImC_{60}) become longer with increasing generation of porphyrinic oligopeptides (with increasing the number of the porphyrin units).[121] Such elongation of the CS

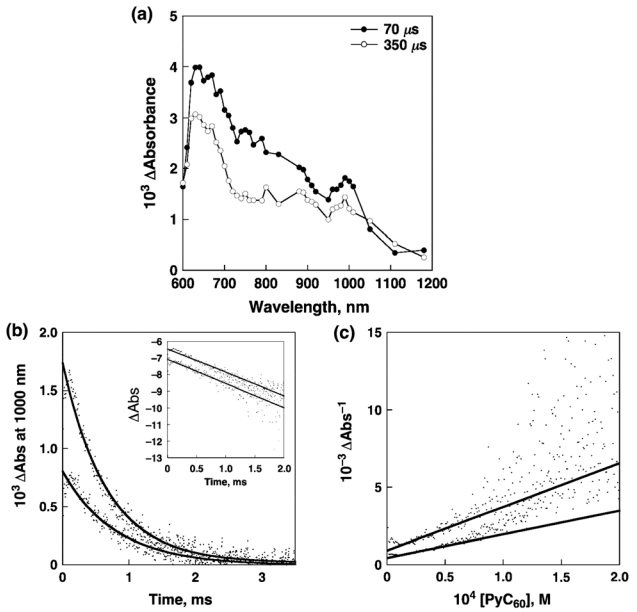

Fig. 16 (a) Transient absorption spectra of $P(ZnP)_8$ (2.9×10^{-6} M) in the presence of PyC_{60} (4.9×10^{-3} M) in deaerated PhCN at 298 K taken at 70 (solid line with black circles) and 350 μs (solid line with white circles) after laser excitation at 561 nm (4 mJ per pulse), respectively. (b) Time profiles of the absorption at 1000 nm due to $PyC_{60}^{\bullet-}$ with different laser powers (4 and 1 mJ per pulse) at 298 K. Inset: first-order plots. (c) Second-order plots.

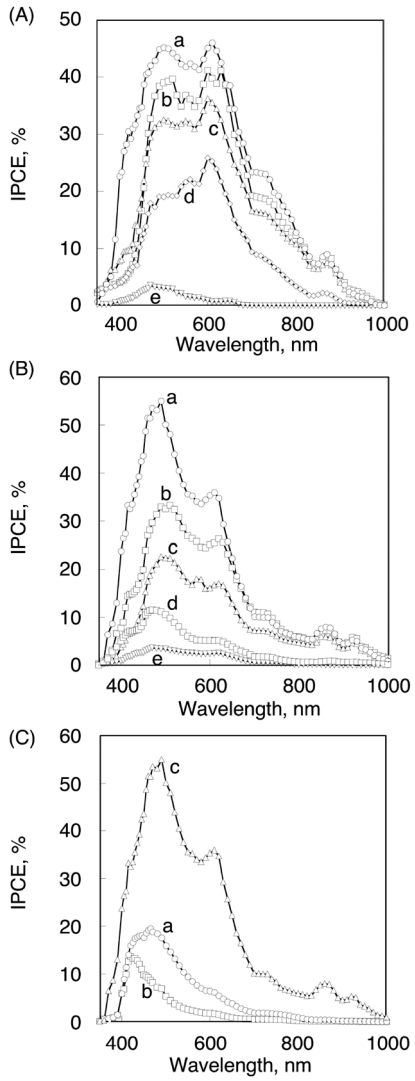

Fig. 17 (A) The photocurrent action spectra (IPCE *vs.* wavelength) of (a) $(P(H_2P)_{16} + C_{60})_m$, (b) $(P(H_2P)_8 + C_{60})_m$, (c) $(P(H_2P)_4 + C_{60})_m$, (d) $(P(H_2P)_2 + C_{60})_m$ and (e) $(P(H_2P)_1 + C_{60})_m$ modified OTE/SnO_2 electrodes. (B) The photocurrent action spectra of (a) $(P(ZnP)_{16} + C_{60})_m$, (b) $(P(ZnP)_8 + C_{60})_m$, (c) $(P(ZnP)_4 + C_{60})_m$, (d) $(P(ZnP)_2 + C_{60})_m$ and (e) $(P(ZnP)_1 + C_{60})_m$ modified electrodes. (C) The photocurrent action spectra of (a) $(P(ZnP)_{16} + ImC_{60})_m$, (b) $(P(ZnP)_{16} + PyC_{60})_m$ and (c) $(P(ZnP)_{16} + C_{60})_m$ modified OTE/SnO_2 electrodes. See text for the employed concentration of the individual species.

lifetimes results from efficient hole migration between the porphyrin units following the photoinduced electron transfer in the supramolecular complexes.

Multiple photosynthetic reaction centres have also been constructed using supramolecular complexes of zinc porphyrin dendrimers [$D(ZnP)_n$: n = 4, 8, 16] with PyC_{60}.[122] Efficient energy migration occurs more efficiently between the ZnP units of dendrimers prior to the photoinduced electron transfer with increasing the generation of dendrimers to attain an extremely long CS lifetime *e.g.*, 0.25 ms for the $D(ZnP)_{16}$–PyC_{60} complex in PhCN at 298 K.[122]

Multiple photosynthetic reaction centres composed of supramolecular complexes of harvesting multiporphyrin units and charge-separation units have enabled us to construct supramolecular organic solar cells by the electrodeposition of mixed porphyrin-peptide oligomers [$P(H_2P)_n$ or $P(ZnP)_n$] and C_{60} clusters [$(P(H_2P)_n + C_{60})_m$ or $(P(ZnP)_n + C_{60})_m$] onto an optically transparent electrode (OTE) of a nanostructured SnO_2 electrode (OTE/SnO_2), to obtain modified electrodes [denoted as $(P(H_2P)_n + C_{60})_m$ or $(P(ZnP)_n + C_{60})_m$ (n = 1, 2, 4, 8, 16)].[123] The IPCE value increased with increasing the number of porphyrins in a polypeptide unit in both $(P(H_2P)_n + C_{60})_m$ and $(P(ZnP)_n + C_{60})_m$ (n = 1, 2, 4, 8, 16) systems as shown in Fig. 17. Such a good photoelectrochemical performance results from efficient photoinduced electron-transfer from the excited state of the porphyrin unit to C_{60} in the supramolecular complex with longer CS lifetimes as the number of porphyrins in a polypeptide unit increases (*vide supra*). The maximum IPCE value of $(P(ZnP)_{16} + C_{60})_m$ (56%) is larger than that of $(P(H_2P)_{16} + C_{60})_m$ (48%) probably because of the larger driving force of the photoinduced electron transfer.

The maximum IPCE values of $(P(ZnP)_{16} + PyC_{60})_m$ (20%) and $(P(ZnP)_{16} + ImC_{60})_m$ (15%) are much smaller than that of $(P(ZnP)_{16} + C_{60})_m$ (56%), whereas the binding constant of $P(ZnP)_{16}$–C_{60} is smaller than those of $P(ZnP)_{16}$–ImC_{60} and $P(ZnP)_{16}$–PyC_{60}.[123] The lower IPCE values of $P(ZnP)_{16}$–ImC_{60} and $P(ZnP)_{16}$–PyC_{60} systems as compared with that of $P(ZnP)_{16}$–C_{60} system may result from the poor electron-transport properties of C_{60} derivatives due to the steric hindrance of the ligand moiety.[123] Thus, a key element for efficient photocurrent generation is mainly the hole and electron transport in

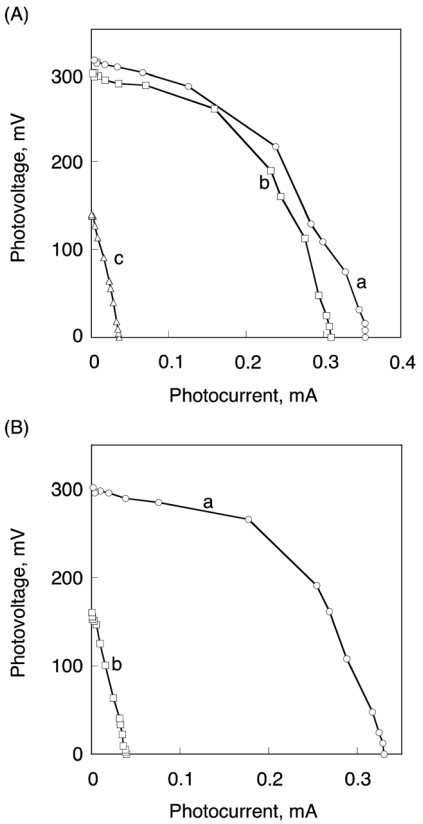

Fig. 18 (A) Current–voltage characteristics of (a) $(P(H_2P)_{16} + C_{60})_m$, (b) $(P(H_2P)_8 + C_{60})_m$, and (c) $(P(H_2P)_1 + C_{60})_m$ modified electrodes. (B) Current–voltage characteristics of (a) $(P(ZnP)_{16} + C_{60})_m$ and (b) $(P(ZnP)_1 + C_{60})_m$. Electrolyte: 0.5 M NaI and 0.01 M I_2 in acetonitrile. Input power: 3.4 mW cm^{-2}, $\lambda > 400$ nm.

the thin film rather than the charge separation between porphyrins and C_{60}.[123]

I/V characteristics of (a) $(P(H_2P)_{16} + C_{60})_m$, (b) $(P(H_2P)_8 + C_{60})_m$ and (c) $(P(H_2P)_1 + C_{60})_m$ modified electrodes under visible light irradiation ($\lambda > 400$ nm) are shown in Fig. 18. The $(P(H_2P)_{16} + C_{60})_m$ system has a larger fill factor (FF) of 0.47, an open circuit voltage (V_{oc}) of 320 mV, a short circuit current density (I_{sc}) of 0.36 mA cm^{-2}, and the overall power conversion efficiency (η) of 1.6% at input power (W_{in}) of 3.4 mW cm^{-2}.[123]

The η values of the $(P(H_2P)_{16} + C_{60})_m$ system was remarkably enhanced (around 40 times) in comparison with the $(P(H_2P)_1 + C_{60})_m$ modified electrode (η = 0.043%) under the same experimental conditions. The η value of $(P(ZnP)_{16} + C_{60})_m$ is also determined as 1.4% and this value is much larger than that of $(P(ZnP)_1 + C_{60})_m$ (0.047%) as shown in Fig. 18B.[123]

6. Conclusions

As described above, porphyrin monomers, dimers, trimers and oligomers form supramolecular complexes with fullerene derivatives *via* electrostatic interactions, π–π interactions and coordination bonds. Photoexcitation of the supramolecular complexes resulted in efficient photoinduced electron transfer from the porphyrin moiety to the fullerene moiety to produce the long-lived CS states as revealed by laser flash photolysis measurements. In particular, a supramolecular complex of a cyclic Ni porphyrin dimer with $Li^+@C_{60}$ [$Li^+@C_{60} \subset Ni_2$-$CPD_{Py}(OC_6)$] affords a long-lived triplet CS state with 0.63 ms lifetime. A high IPCE value (77% at 450 nm) was achieved for a supramolecular solar cell using the OTE/SnO_2/($ZnTPPS^{4-}$/$Li^+@C_{60})_n$ electrode. The use of porphyrin oligomer peptides has also enabled to construct multiple photosynthetic reaction centres composed of light-harvesting multiporphyrin units and charge-separation units linked by both the coordination bond and π–π interactions, which afforded long-lived CS states. Supramolecular organic solar cells composed of porphyrinic oligopeptides and C_{60} exhibited higher overall power conversion efficiency with increasing the number of porphyrin units. Supramolecular complexes formed between porphyrins and fullerenes in particular $Li^+@C_{60}$ provide promising materials for more efficient solar energy conversion.

Acknowledgements

The authors gratefully acknowledge the contributions of their collaborators and co-workers mentioned in the cited references, in particular Prof. Fumito Tani (Kyushu University) and Prof. Taku Hasobe (Keio University). Financial supports from the Grants-in-Aid (no. 20108010 to S.F. and 23750014 to K.O.) from MEXT of Japan and KOSEF/MEST of Korea through WCU project (R31-2008-000-10010-0) are gratefully acknowledged.

References

1 *Anoxygenic Photosynthetic Bacteria*, ed. R. E. Blankenship, M. T. Madigan and C. E. Bauer, Kluwer Academic Publishers, Dordrecht, The Netherlands, 1995.
2 W. Leibl and P. Mathis, in *Electron Transfer in Photosynthesis. Series on Photoconversion of Solar Energy*, 2004, vol. 2, p. 117.
3 T. A. Faunce, W. Lubitz, A. W. Rutherford, D. MacFarlane, G. F. Moore, P. Yang, D. G. Nocera, T. A. Moore, D. H. Gregory, S. Fukuzumi, K. B. Yoon, F. A. Armstrong, M. R. Wasielewski and S. Styring, *Energy Environ. Sci.*, 2013, **6**, 695.
4 S. Fukuzumi, Y. Yamada, T. Suenobu, K. Ohkubo and H. Kotani, *Energy Environ. Sci.*, 2011, **4**, 2754.
5 A. Harriman and J.-P. Sauvage, *Chem. Soc. Rev.*, 1996, **25**, 41.
6 M. N. Paddon-Row, *Adv. Phys. Org. Chem.*, 2003, **38**, 1.
7 M. N. Paddon-Row, *Acc. Chem. Res.*, 1994, **27**, 18.
8 D. Gust, T. A. Moore and A. L. Moore, *Acc. Chem. Res.*, 2009, **42**, 1890.
9 D. Gust, T. A. Moore and A. L. Moore, *Faraday Discuss.*, 2012, **155**, 9.
10 M. R. Wasielewski, *Acc. Chem. Res.*, 2009, **42**, 1910.
11 C. Thilgen and F. Diederich, *Chem. Rev.*, 2006, **106**, 5049.
12 F. Giacalone and N. Martín, *Chem. Rev.*, 2006, **106**, 5136.

13 W.-S. Li and T. Aida, *Chem. Rev.*, 2009, **109**, 6047.
14 C. M. Drain, A. Varotto and I. Radivojevic, *Chem. Rev.*, 2009, **109**, 1630.
15 (*a*) F. D'Souza and O. Ito, *Coord. Chem. Rev.*, 2005, **249**, 1410; (*b*) F. D'Souza and O. Ito, *Chem. Commun.*, 2009, 4913; (*c*) F. D'Souza, A. S. D. Sandanayaka and O. Ito, *J. Phys. Chem. Lett.*, 2010, **1**, 2586; (*d*) F. D'Souza and O. Ito, *Chem. Soc. Rev.*, 2012, **41**, 86.
16 (*a*) S. Fukuzumi, *Bull. Chem. Soc. Jpn.*, 2006, **79**, 177; (*b*) S. Fukuzumi, *Phys. Chem. Chem. Phys.*, 2008, **10**, 2283; (*c*) S. Fukuzumi, *Pure Appl. Chem.*, 2007, **79**, 981; (*d*) S. Fukuzumi, *Org. Biomol. Chem.*, 2003, **1**, 609.
17 H. Imahori and S. Fukuzumi, *Adv. Funct. Mater.*, 2004, **14**, 525.
18 D. M. Guldi, G. M. A. Rahman, F. Zerbetto and M. Prato, *Acc. Chem. Res.*, 2005, **38**, 871.
19 G. Bottari, G. de la Torre, D. M. Guldi and T. Torres, *Chem. Rev.*, 2010, **110**, 676.
20 S. Fukuzumi, T. Honda, K. Ohkubo and T. Kojima, *Dalton Trans.*, 2009, 3880.
21 S. Fukuzumi and T. Kojima, *J. Mater. Chem.*, 2008, **18**, 1427.
22 D. M. Guldi and V. Sgobba, *Chem. Commun.*, 2011, **47**, 606.
23 D. M. Guldi, *Phys. Chem. Chem. Phys.*, 2007, **9**, 1400.
24 S. Fukuzumi and K. Ohkubo, *J. Mater. Chem.*, 2012, **22**, 4575.
25 (*a*) K. Ohkubo and S. Fukuzumi, *J. Porphyrins Phthalocyanines*, 2008, **12**, 993; (*b*) K. Ohkubo and S. Fukuzumi, *Bull. Chem. Soc. Jpn.*, 2009, **82**, 303.
26 G. Bottari, G. de la Torre, D. M. Guldi and T. Torres, *Chem. Rev.*, 2010, **110**, 6768.
27 M. V. Martinez-Diaz, N. S. Fender, M. S. Rodriguez-Morgade, M. Gomez-Lopez, F. Diederich, L. Echegoyen, J. F. Stoddart and T. Torres, *J. Mater. Chem.*, 2002, **12**, 2095.
28 (*a*) C. G. Claessens and T. Torres, *Chem. Commun.*, 2004, 1298; (*b*) C. G. Claessens and T. Torres, *J. Am. Chem. Soc.*, 2002, **124**, 14522.
29 S. Fukuzumi, K. Ohkubo, F. D'Souza and J. L. Sessler, *Chem. Commun.*, 2012, **48**, 9801.
30 J.-F. Nierengarten, U. Hahn, T. M. F. Duarte, F. Cardinali, N. Solladié, M. E. Walther, A. Van Dorsselaer, H. Herschbach, E. Leize, A.-M. Albrecht-Gary, A. Trabolsi and M. Elhabiri, *C. R. Chim.*, 2006, **9**, 1022.
31 L. Echegoyen, F. Diederich and L. E. Echegoyen, in *Fullerenes: Chemistry, Physics and Technology*, ed. K. M. Kadish and R. S. Ruoff, Wiley-Interscience, New York, 2000, pp. 1–51.
32 T. M. Figueira-Duarte, A. Gegout and J.-F. Nierengarten, *Chem. Commun.*, 2007, 109.
33 S. Fukuzumi and D. M. Guldi, in *Electron Transfer in Chemistry*, ed. V. Balzani, Wiley-VCH, Weinheim, 2001, vol. 2, pp. 270–337.
34 S. Fukuzumi, in *Functional Organic Materials*, ed. T. J. J. Müller and U. H. F. Bunz, Wiley-VCH, 2007, pp. 465–510.
35 J.-F. Nierengarten, *New J. Chem.*, 2004, **28**, 1177.
36 S. Fukuzumi, I. Nakanishi, T. Suenobu and K. M. Kadish, *J. Am. Chem. Soc.*, 1999, **121**, 3468.
37 S. Fukuzumi, K. Ohkubo, H. Imahori and D. M. Guldi, *Chem.–Eur. J.*, 2003, **9**, 1585.
38 Y. Kawashima, K. Ohkubo and S. Fukuzumi, *J. Phys. Chem. A*, 2013, **117**, 6737.
39 S. Fukuzumi, K. Ohkubo, H. Imahori, J. Shao, Z. Ou, G. Zheng, Y. Chen, R. K. Pandey, M. Fujitsuka, O. Ito and K. M. Kadish, *J. Am. Chem. Soc.*, 2001, **123**, 10676.
40 D. Wróbel and A. Graja, *Coord. Chem. Rev.*, 2011, **255**, 2555.
41 H. Imahori, K. Tamaki, D. M. Guldi, C. Luo, M. Fujitsuka, O. Ito, Y. Sakata and S. Fukuzumi, *J. Am. Chem. Soc.*, 2001, **123**, 2607.
42 H. Imahori, D. M. Guldi, K. Tamaki, Y. Yoshida, C. Luo, Y. Sakata and S. Fukuzumi, *J. Am. Chem. Soc.*, 2001, **123**, 6617.
43 K. Ohkubo, H. Imahori, J. Shao, Z. Ou, K. M. Kadish, Y. Chen, G. Zheng, R. K. Pandey, M. Fujitsuka, O. Ito and S. Fukuzumi, *J. Phys. Chem. A*, 2002, **106**, 10991.
44 H. Imahori, K. Tamaki, Y. Araki, Y. Sekiguchi, O. Ito, Y. Sakata and S. Fukuzumi, *J. Am. Chem. Soc.*, 2002, **124**, 5165.
45 K. Ohkubo, H. Kotani, J. Shao, Z. Ou, K. M. Kadish, G. Li, R. K. Pandey, M. Fujitsuka, O. Ito, H. Imahori and S. Fukuzumi, *Angew. Chem., Int. Ed.*, 2004, **43**, 853.
46 F. D'Souza, P. M. Smith, M. E. Zandler, A. L. McCarty, M. Itou, Y. Araki and O. Ito, *J. Am. Chem. Soc.*, 2004, **126**, 7898.
47 H. Imahori, Y. Sekiguchi, Y. Kashiwagi, T. Sato, Y. Araki, O. Ito, H. Yamada and S. Fukuzumi, *Chem.–Eur. J.*, 2004, **10**, 3184.
48 F. D'Souza, R. Chitta, S. Gadde, S. D.-M. Islam, A. L. Schumacher, M. E. Zandler, Y. Araki and O. Ito, *J. Phys. Chem. B*, 2006, **110**, 25240.
49 F. D'Souza, R. Chitta, S. Gadde, L. M. Rogers, P. A. Karr, M. E. Zandler, A. S. D. Sandanayaka, Y. Araki and O. Ito, *Chem.–Eur. J.*, 2007, **13**, 916.
50 R. Chitta, K. Ohkubo, M. Tasior, N. K. Subbaiyan, M. E. Zandler, D. T. Gryko, S. Fukuzumi and F. D'Souza, *J. Am. Chem. Soc.*, 2008, **130**, 14263.
51 F. D'Souza, E. Maligaspe, P. A. Karr, A. L. Schumacher, M. El Ojaimi, C. P. Gros, J.-M. Barbe, K. Ohkubo and S. Fukuzumi, *Chem.–Eur. J.*, 2008, **14**, 674.
52 F. D'Souza, E. Maligaspe, K. Ohkubo, M. E. Zandler, N. K. Subbaiyan and S. Fukuzumi, *J. Am. Chem. Soc.*, 2009, **131**, 8787.
53 F. D'Souza, G. M. Venukadasula, K. Yamanaka, N. K. Subbaiyan, M. E. Zandler and O. Ito, *Org. Biomol. Chem.*, 2009, **7**, 1076.
54 F. D'Souza, N. K. Subbaiyan, Y. Xie, J. P. Hill, K. Ariga, K. Ohkubo and S. Fukuzumi, *J. Am. Chem. Soc.*, 2009, **131**, 16138.
55 E. Maligaspe, T. Kumpulainen, N. K. Subbaiyan, M. E. Zandler, H. Lemmetyinen, N. V. Tkachenko and F. D'Souza, *Phys. Chem. Chem. Phys.*, 2010, **12**, 7434.

56 M. E. El-Khouly, D. K. Ju, K.-Y. Kay, F. D'Souza and S. Fukuzumi, *Chem.–Eur. J.*, 2010, **16**, 6193.
57 F. D'Souza, C. A. Wijesinghe, M. E. El-Khouly, J. Hudson, M. Niemi, H. Lemmetyinen, N. V. Tkachenko, M. E. Zandler and S. Fukuzumi, *Phys. Chem. Chem. Phys.*, 2011, **13**, 18168.
58 F. D'Souza, A. N. Amin, M. E. El-Khouly, N. K. Subbaiyan, M. E. Zandler and S. Fukuzumi, *J. Am. Chem. Soc.*, 2012, **134**, 654.
59 S.-H. Lee, A. G. Larsen, K. Ohkubo, J. R. Reimers, S. Fukuzumi and M. J. Crossley, *Chem. Sci.*, 2012, **3**, 257.
60 V. Garg, G. Kodis, M. Chachisvilis, M. Hambourger, A. L. Moore, T. A. Moore and D. Gust, *J. Am. Chem. Soc.*, 2011, **133**, 2944.
61 J. Frey, G. Kodis, S. D. Straight, T. A. Moore, A. L. Moore and D. Gust, *J. Phys. Chem. A*, 2013, **117**, 607.
62 Y. Kashiwagi, K. Ohkubo, J. A. McDonald, I. M. Blake, M. J. Crossley, Y. Araki, O. Ito, H. Imahori and S. Fukuzumi, *Org. Lett.*, 2003, **5**, 2719.
63 D. Curiel, K. Ohkubo, J. R. Reimers, S. Fukuzumi and M. J. Crossley, *Phys. Chem. Chem. Phys.*, 2007, **9**, 5260.
64 J. Iehl, M. Vartanian, M. Holler, J.-F. Nierengarten, B. Delavaux-Nicot, J.-M. Strub, A. Van Dorsselaer, Y. Wu, J. Mohanraj, K. Yoosaf and N. Armaroli, *J. Mater. Chem.*, 2011, **21**, 1562.
65 F. D'Souza, G. R. Deviprasad, M. S. Rahman and J.-P. Choi, *Inorg. Chem.*, 1999, **38**, 2157.
66 F. D'Souza, G. R. Deviprasad, M. E. Zandler, V. T. Hoang, A. Klykov, M. VanStipdonk, A. Perera, M. E. El-Khouly, M. Fujitsuka and O. Ito, *J. Phys. Chem. A*, 2002, **106**, 3243.
67 T. Da Ros, M. Prato, D. M. Guldi, M. Ruzzi and L. Pasimeni, *Chem.–Eur. J.*, 2001, **7**, 816.
68 F. D'Souza, G. R. Deviprasad, M. E. El-Khouly, M. Fujitsuka and O. Ito, *J. Am. Chem. Soc.*, 2001, **123**, 5277.
69 T. Honda, T. Nakanishi, K. Ohkubo, T. Kojima and S. Fukuzumi, *J. Am. Chem. Soc.*, 2010, **132**, 10155.
70 T. Honda, T. Kojima, N. Kobayashi and S. Fukuzumi, *Angew. Chem., Int. Ed.*, 2011, **50**, 2725.
71 S. Fukuzumi, T. Honda and T. Kojima, *Coord. Chem. Rev.*, 2012, **256**, 2488.
72 J. L. Sessler, E. Karnas, S. K. Kim, Z. Ou, M. Zhang, K. M. Kadish, K. Ohkubo and S. Fukuzumi, *J. Am. Chem. Soc.*, 2008, **130**, 15256.
73 E. Karnas, S. K. Kima, K. A. Johnson, J. L. Sessler, K. Ohkubo and S. Fukuzumi, *J. Am. Chem. Soc.*, 2010, **132**, 16617.
74 S. Aoyagi, E. Nishibori, H. Sawa, K. Sugimoto, M. Takata, Y. Miyata, R. Kitaura, H. Shinohara, H. Okada, T. Sakai, Y. Ono, K. Kawachi, K. Yokoo, S. Ono, K. Omote, Y. Kasama, S. Ishikawa, T. Komuro and H. Tobita, *Nat. Chem.*, 2010, **4**, 678.
75 S. Fukuzumi, K. Ohkubo, Y. Kawashima, D. S. Kim, J. S. Park, A. Jana, V. Lynch, D. Kim and J. L. Sessler, *J. Am. Chem. Soc.*, 2011, **133**, 15938.
76 N. L. Bill, M. Ishida, S. Bähring, J. M. Lim, S. Lee, C. M. Davis, V. M. Lynch, K. A. Nielsen, J. O. Jeppesen, K. Ohkubo, S. Fukuzumi, D. Kim and J. L. Sessler, *J. Am. Chem. Soc.*, 2013, **135**, 10852.
77 Y. Kawashima, K. Ohkubo and S. Fukuzumi, *J. Phys. Chem. A*, 2012, **116**, 8942.
78 K. Ohkubo, Y. Kawashima and S. Fukuzumi, *Chem. Commun.*, 2012, **48**, 4314.
79 J. S. Park, E. Karnas, K. Ohkubo, P. Chen, K. M. Kadish, S. Fukuzumi, C. W. Bielawski, T. W. Hudnall, V. M. Lynch and J. L. Sessler, *Science*, 2010, **329**, 1324.
80 M. Murakami, K. Ohkubo, T. Nanjo, K. Souma, N. Suzuki and S. Fukuzumi, *ChemPhysChem*, 2010, **11**, 2594.
81 K. Ohkubo, Y. Kawashima, H. Sakai, T. Hasobe and S. Fukuzumi, *Chem. Commun.*, 2013, **49**, 4474.
82 T. Hasobe, Y. Kashiwagi, M. A. Absalom, J. Sly, K. Hosomizu, M. J. Crossley, H. Imahori, P. V. Kamat and S. Fukuzumi, *Adv. Mater.*, 2004, **16**, 975.
83 T. Hasobe, H. Imahori, S. Fukuzumi and P. V. Kamat, *J. Phys. Chem. B*, 2003, **107**, 12105.
84 T. Hasobe, H. Imahori, P. V. Kamat, T. K. Ahn, D. Kim, T. Hanada, T. Hirakawa and S. Fukuzumi, *J. Am. Chem. Soc.*, 2005, **127**, 1216.
85 T. Hasobe, P. V. Kamat, V. Troiani, N. Solladié, T. K. Ahn, S. K. Kim, D. Kim, A. Kongkanand, S. Kuwabata and S. Fukuzumi, *J. Phys. Chem. B*, 2005, **109**, 19.
86 D. Sun, F. S. Tham, C. A. Reed, L. Chaker, M. Burgess and P. D. W. Boyd, *J. Am. Chem. Soc.*, 2000, **122**, 10704.
87 D. Sun, F. S. Tham, C. A. Reed, L. Chaker and P. D. W. Boyd, *J. Am. Chem. Soc.*, 2002, **124**, 6604.
88 M. Tanaka, K. Ohkubo, C. P. Gros, R. Guilard and S. Fukuzumi, *J. Am. Chem. Soc.*, 2006, **128**, 14625.
89 L. P. Hernández-Eguía, E. C. Escudero-Adán, I. C. Pintre, B. Ventura, L. Flamigni and P. Ballester, *Chem.–Eur. J.*, 2011, **17**, 14564.
90 A. L. Kieran, S. I. Pascu, T. Jarrosson and J. K. M. Sanders, *Chem. Commun.*, 2005, 1276.
91 B. Grimm, J. Schornbaum, C. M. Cardona, J. D. van Paauwe, P. D. W. Boyd and D. M. Guldi, *Chem. Sci.*, 2011, **2**, 1530.
92 L. P. Hernández-Eguía, E. C. Escudero-Adán, J. R. Pinzón, L. Echegoyen and P. Ballester, *J. Org. Chem.*, 2011, **76**, 3258.
93 S. K. Samanta and M. Schmittel, *Org. Biomol. Chem.*, 2013, **11**, 3108.
94 K. Börjesson, J. G. Woller, E. Parsa, J. Mårtensson and B. Albinsson, *Chem. Commun.*, 2012, **48**, 1793.
95 B. Kang, R. K. Totten, M. H. Weston, J. T. Hupp and S. T. Nguyen, *Dalton Trans.*, 2012, **41**, 12156.
96 S. Fukuzumi, I. Amasaki, K. Ohkubo, C. P. Gros, R. Guilard and J.-M. Barbe, *RSC Adv.*, 2012, **2**, 3741.
97 H. Nobukuni, F. Tani, Y. Shimazaki, Y. Naruta, K. Ohkubo, T. Nakanishi, T. Kojima, S. Fukuzumi and S. Seki, *J. Phys. Chem. C*, 2009, **113**, 19694.
98 T. Yamaguchi, N. Ishii, K. Tashiro and T. Aida, *J. Am. Chem. Soc.*, 2003, **125**, 13934.

99 R. Harada, Y. Matsuda, H. Okawa and T. Kojima, *Angew. Chem., Int. Ed.*, 2004, **43**, 1825.
100 T. Kojima, T. Nakanishi, R. Harada, K. Ohkubo, S. Yamauchi and S. Fukuzumi, *Chem.–Eur. J.*, 2007, **13**, 8714.
101 T. Nakanishi, T. Kojima, K. Ohkubo, T. Hasobe, K. Nakayama and S. Fukuzumi, *Chem. Mater.*, 2008, **20**, 7492.
102 T. Kojima, R. Harada, T. Nakanishi, K. Kaneko and S. Fukuzumi, *Chem. Mater.*, 2007, **19**, 51.
103 A. Saeki, Y. Koizumi, T. Aida and S. Seki, *Acc. Chem. Res.*, 2012, **45**, 1193.
104 R. J. O. M. Hoofman, M. P. de Hass, L. D. A. Siebbeles and J. M. Warman, *Nature*, 1998, **392**, 54.
105 J. H. Choi, T. Honda, S. Seki and S. Fukuzumi, *Chem. Commun.*, 2011, **47**, 11213.
106 E. Frankevich, Y. Maruyama and H. Ogata, *Chem. Phys. Lett.*, 1993, **214**, 39.
107 H. Nobukuni, Y. Shimazaki, H. Uno, Y. Naruta, K. Ohkubo, T. Kojima, S. Fukuzumi, S. Seki, H. Sakai, T. Hasobe and F. Tani, *Chem.–Eur. J.*, 2010, **16**, 11611.
108 T. Kamimura, K. Ohkubo, Y. Kawashima, H. Nobukuni, Y. Naruta, F. Tani and S. Fukuzumi, *Chem. Sci.*, 2013, **4**, 1451.
109 F. D'Souza, P. M. Smith, S. Gadde, A. L. McCarty, M. J. Kullman, M. E. Zandler, M. Itou, Y. Araki and O. Ito, *J. Phys. Chem. B*, 2004, **108**, 11333.
110 N. Armaroli, F. Diederich, L. Echegoyen, T. Habicher, L. Flamigni, G. Marconi and J.-F. Nierengarten, *New J. Chem.*, 1999, 77.
111 T. Da Ros, M. Prato, D. M. Guldi, E. Alessio, M. Ruzzi and L. Pasimeni, *Chem. Commun.*, 1999, 635.
112 F. Hauke, A. Swartz, D. M. Guldi and A. Hirsch, *J. Mater. Chem.*, 2002, **12**, 2088.
113 A. Takai, M. Chkounda, A. Eggenspiller, C. P. Gros, M. Lachkar, J.-M. Barbe and S. Fukuzumi, *J. Am. Chem. Soc.*, 2010, **132**, 4477.
114 F. D'Souza, G. R. Deviprasad, M. E. Zandler, V. T. Hoang, A. Klykov, M. VanStipdonk, A. Perera, M. E. El-Khouly, M. Fujitsuka and O. Ito, *J. Phys. Chem. A*, 2002, **106**, 3243.
115 D. I. Schuster, K. Loa, D. M. Guldi, A. Palkar, L. Echegoyen, C. Stanisky, R. J. Cross, M. Niemi, M. V. Tkachenko and H. Lemmetyinen, *J. Am. Chem. Soc.*, 2007, **129**, 15973.
116 A. Takai, C. P. Gros, R. Guilard and S. Fukuzumi, *Chem.–Eur. J.*, 2009, **15**, 3110.
117 A. Takai, C. P. Gros, J.-M. Barbe and S. Fukuzumi, *Chem.–Eur. J.*, 2011, **17**, 3420.
118 A. Takai, C. P. Gros, J.-M. Barbe and S. Fukuzumi, *Phys. Chem. Chem. Phys.*, 2010, **12**, 12160.
119 N. Solladié, A. Hamel and M. Gross, *Tetrahedron Lett.*, 2000, **41**, 6075.
120 F. Aziat, R. Rein, J. Peon, E. Rivera and N. Solladié, *J. Porphyrins Phthalocyanines*, 2008, **12**, 1232.
121 S. Fukuzumi, K. Saito, K. Ohkubo, V. Troiani, H. Qiu, S. Gadde, F. D'Souza and N. Solladié, *Phys. Chem. Chem. Phys.*, 2011, **13**, 17019.
122 S. Fukuzumi, K. Saito, K. Ohkubo, T. Khoury, Y. Kashiwagi, M. A. Absalom, S. Gadde, F. D'Souza, Y. Araki, O. Ito and M. J. Crossley, *Chem. Commun.*, 2011, **47**, 7980.
123 T. Hasobe, K. Saito, P. V. Kamat, V. Troiani, H. Qiu, N. Solladié, T. K. Ahn, K. S. Kim, S. K. Kim, D. Kim, F. D'Souza and S. Fukuzumi, *J. Mater. Chem.*, 2007, **17**, 4160.

